Advances in Nano Research, *Vol. 14, No. 4 (2023) 303-312*
https://doi.org/10.12989/anr.2023.14.4.303

Simply supported boundary condition for bifurcation analysis of functionally graded material: Thickness control by exponential fraction law

Shadi Alghaffari[1], Muzamal Hussain*[2], Mohamed A. Khadimallah[3], Faisal Al Thobiani[4] and Hussain Talat Sulaimani[1]

[1]*Department of Port and Maritime Transportation, Faculty of Maritime Studies, King Abdul Aziz University- Jeddah-KSA*
[2]*Department of Mathematics, Govt. College University Faisalabad, 38000, Faisalabad, Pakistan*
[3]*Department of Civil Engineering, College of Engineering in Al-Kharj, Prince Sattam Bin Abdulaziz University, Al-Kharj, 11942, Saudi Arabia*
[4]*Department of Marine Engineering, Faculty of Maritime Studies, King Abdul Aziz University- Jeddah-KSA*

(*Received November 2, 2021, Revised November 8, 2022, Accepted November 17, 2022*)

Abstract. In this study, the bifurcation analysis of functionally graded material is done using exponential volume fraction law. Shell theory of Love is used for vibration of shell. The Galerkin's method is applied for the formation of three equations in eigen value form. This eigen form gives the frequencies using the computer software MATLAB. The variations of natural frequencies (Hz) for Type-I and Type-II functionally graded cylindrical shells are plotted for exponential volume fraction law. The behavior of exponent of volume fraction law is seen for three different values. Moreover, the frequency variations of Type-I and -II clamped simply supported FG cylindrical shell with different positions of ring supports against the circumferential wave number are investigated. The procedure adopted here enables to study vibration for any boundary condition but for brevity, numerical results for a cylindrical shell with clamped simply supported edge condition are obtained and their analysis with regard various physical parameters is done.

Keywords: clamped simply supported; cylindrical shell; exponential volume fraction; thickness; type-I and –II

1. Introduction

The vibrations of thin circular cylindrical shells were checked by Sharma (1974, 1979). In his work characteristics beam functions was used to evaluate axial deformation functions. After that he applied Rayleigh-Ritz method to observe shell vibration characteristics. In the applied method Lagrange functional was employed for the vibration amplitudes and axial deformation functions. A proper energy functional was minimized to calculate this method and it was minimized with respect to vibration amplitude coefficients. Selection of these presumed functions were made to satisfy geometric conditions for a cylindrical shell problem. Greif and Chung (1975) analyzed the vibrations of a cylindrical shell under various end conditions with several intermediate constraints between the ends.

They used Rayleigh-Ritz procedure with the axial modal displacement in the form of Fourier series expression.

Ludwig and Krieg (1981) utilized an adaptive approach to establish the frequencies and periods of thin cylindrical shells, using the shell theory of Flugge. To enhance the stability and strength of cylindrical shells, Loy and Lam (1997) studied influence of ring supports on cylindrical shell vibrations. Loy *et al*. (1999) studied vibrations of functionally graded cylindrical shells and influence of functionally graded material composition was examined. Amabili (1999) examined free vibration characteristics of cylindrical shells and tubes containing thick fluid. Akbaş (2017a, b) investigated the free vibration analysis of edge cracked cantilever microscale beams composed of functionally graded material (FGM) based on the modified couple stress theory (MCST). The material properties of the beam are assumed to change in the height direction according to the exponential distribution. The FG nanobeam is excited by a transverse triangular force impulse modulated by a harmonic motion. Mechanical properties of FG beam depends on the position. The Kelvin–Voigt model is considered in the damping effect. In solution of the dynamic problem, finite element method is used within Timoshenko beam theory. Shahmohammadi *et al*. (2020) presented the free vibration analysis of shell panels made of functionally graded material (FGM) in the form of the ordinary and sandwich FGM and laminated shells using the isogeometric B3-spline finite strip method (IG-SFSM). B3-spline and Lagrangian interpolation are employed along the longitudinal and transverse directions respectively in this type of finite strip.

Swaddiwudhpong *et al*. (1995) analyzed vibrations of cylindrical shells with intermediate supports. They applied a mechanized Raleigh-Ritz technique to find out the shell frequencies and the respective mode shapes of cylindrical shells with central supports. This is a particular type of ring-stiffened cylinder wherein the rings were largely inflexible or when tight ring supports are extended in between the two supported edges. Ritz polynomial functions were considered for the axial modal dependence and were contained numerous end conditions with any number of intermediate supports. This was done to raise the powers of

*Corresponding author, Assistant Professor, Ph.D.,
E-mail: muzamal45@gmail.com

ISSN: 2287-237X (Print), 2287-2388 (Online)

the parameters so that any essential boundary condition can be met. This procedure was easy to code that needed a computer program to get numerical results for cylindrical shells with different boundary conditions. The pronounced effects of central supports on the shell frequencies were discussed and the results were demonstrated in graphical forms for comparing with those found by mechanical engineers. Arefi and Żur (2020) investigated the free vibration analysis of a functionally graded cylindrical nanoshell resting on Pasternak foundation is presented based on the nonlocal elasticity theory. A two-dimensional formulation along the axial and radial directions is presented based on the first-order shear deformation shell theory. Hamilton's principle is employed for derivation of the governing equations of motion. Akbaş (2016a, b) studied the forced vibration analysis of a simple supported viscoelastic nanobeam based on modified couple stress theory (MCST). The nanobeam is excited by a transverse triangular force impulse modulated by a harmonic motion. The elastic medium is considered as Winkler-Pasternak elastic foundation. The damping effect is considered by using the Kelvin–Voigt viscoelastic model. The cracked beam is modelled using a proper modification of the classical cracked-beam theory consisting of two sub-beams connected through a massless elastic rotational spring. Koochi and Goharimanesh (2021) studied the nonlinear oscillation of carbon nanotube manufactured nano-resonator. The governing equation of the nano-resonator is extracted in the context of the nonlocal elasticity. The impact of the Casimir force is also incorporated in the developed model. A closed-form solution based on the energy balance method is presented for investigating the oscillations of the nano-resonator. Civalek (2020) presented the free vibration characteristics of thick skew plates reinforced by functionally graded carbon nanotubes (CNTs) reinforced composite. Discrete singular convolution (DSC) method is used for the numerical solution of vibration problems via geometric mapping technique. Using the geometric transformation via a four-node element, the straight-sided quadrilateral physical domain is mapped into a square domain in the computational space.

Sharma *et al*. (1998) computed natural frequencies of fluid filled cylindrical shells. The axial modal deformation displacement functions were measured by trigonometric functions in the Fourier series expressions. Wang and Lai (2000) determined the natural frequencies for a finite length circular cylindrical shell with a number of boundary conditions. Civalek and Jalaei (2020) studied a geometric transformation method based on discrete singular convolution (DSC) to solve the buckling problem of a functionally graded carbon nanotube (FG-CNT)-reinforced composite skew plate. The straight-sided quadrilateral plate geometry is mapped into a square domain in the computational space using a four-node DSC transformation method. Ergin and Temarel (2002) scrutinized the vibration of horizontally and partially filled and submerged cylindrical shells. The fluid was regarded to be perfect and its forces were well-tied with the inertial forces termed as: "the pressure of the fluid on the damped surface of the shell in phase with the shell structural acceleration". Standard finite element methods were employed to determine the response in vacuum motion character of cylindrical shells. It was also noted that the shell structure maintained its mode forms in vacuum when it was related with the adjacent fluid and that every mode form raised to pressure supply of interrelated surface of cylindrical shells. Akbaş (2020) investigated the axially damped forced vibration responses of viscoelastic nanorods within the frame of the modal analysis. The nonlocal elasticity theory is used in the constitutive relation of the nanorod with the Kelvin-Voigt viscoelastic model. In the forced vibration problem, a cantilever nanorod subjected to a harmonic load at the free end of the nanorod is considered in the numerical examples. Bing *et al*. (2005) determined natural frequencies of thin sheeted cylindrical shells for a various end conditions. Donnell shell theory was used for shell dynamical equations and the wave propagation approach was employed to solve these equations. All the mode forms were graphed to articulate the circumferential and axial wave numbers (n, m). They used numerical method to calculate the natural frequencies and the results were compared to those found by using (FEM). So that consistency of theoretical solutions was established. The consequence of associated factors on natural frequencies was observed in detail which exhibited validity, robustness and accuracy of the technique for long thin cylindrical shells. Akbaş (2019) presented axially forced vibration of a cracked nanorod under harmonic external dynamically load. In constitutive equation of problem, the nonlocal elasticity theory is used. The Crack is modelled as an axial spring in the crack section. In the axial spring model, the nonrod separates two sub-nanorods and the flexibility of the axial spring represents the effect of the crack. Boundary condition of the nanorod is selected as fixed-free and a harmonic load is subjected at the free end of the nanorod. Aboueregal and Sedighi (2021) presented contribution aims to address a problem of thermovisco-elasticity for the analysis of the transition temperature and thermal stresses in an infinitely circular annular cylinder. The inner surface is traction-free and subjected to thermal shock heating, while the outer surface is thermally insulated and free of traction. Akbaş (2018a, b) investigated the forced vibration analysis of a cracked functionally graded microbeam using modified couple stress theory with damping effect. Mechanical properties of the functionally graded beam change vary along the thickness direction. The crack is modelled with a rotational spring. The Kelvin-Voigt model is considered in the damping effect. Static bending of an edge cracked cantilever nanobeam composed of functionally graded material (FGM) subjected to transversal point load at the free end of the beam is investigated based on modified couple stress theory. Material properties of the beam change in the height direction according to exponential distributions. Zhang *et al.* (2006) applied a procedure for a precise vibration study of cylindrical shells and used the differential quardrature method to solve shell dynamical equations. The process was engaged to restrict the interpolating base functions. All the shell dynamical equations were obtained by Goldenveizer-Novozhilov shell approximations. A suitable arrangement of the exterior points was made so as to unite the discretized edge situation with the recognized differential equations. By the application of efficiently supported interpolating basis functions wellformed and lined matrices were acquired which made easy wide calculations. Extraneous eigen-

values were evaded by applying end condition with exterior mesh points. Wide-ranging formulation was made for handling different shell end conditions. A comparison of results was made with already measured results in literature to find the competence and consistency of the present technique. By using the small mesh points with exterior points to control edge conditions the exact natural frequencies can be obtained. Abouelregal *et al*. (2021) investigated the thermal and mechanical vibration properties of functionally graded microbeams. The governing system of equations is formulated on the basis of classical Euler–Bernoulli beam model incorporating the generalized dual-phase lag model of thermoelasticity rather than the conventional steady-state Fourier heat conduction.

Lee and Chang (2009) gave a numerical study of coupled problems of fluid conveying dual walled carbon annotates and examined the effects of characteristic ratio and Van der Waals forces on basic frequencies. Akbaş (2018c) presented the forced vibration responses of a cantilever nanobeam with crack using modified couple stress theory with damping effect. The crack is modeled with a rotational spring. The Kelvin–Voigt model is considered in the damping effect. In solution of the dynamic problem, finite element method is used within Timoshenko beam theory in the time domain. Influences of the geometry, crack and material parameters on forced vibration responses of cracked nanobeams are examined and discussed. Jena *et al*. (2020) studied the vibration characteristics of functionally graded porous nanobeam embedded in an elastic substrate of Winkler–Pasternak type. Classical beam theory or Euler–Bernoulli beam theory has been incorporated to address the displacement of the FG nanobeam. bi-Helmholtz type of nonlocal elasticity is being used to capture the small scale effect of the FG nanobeam.

Sarkheil *et al*. (2016) investigated the oscillation of bi-layered cylindrical shells composed of two distinct materials using Sander's thin shell theory. Recently some researcher used different methods for nonlinear modeling (Eltaher *et al*. 2019, Ebrahimi *et al*. 2019, Safaei *et al*. 2019, Shahsavari *et al*. 2019, Benmansour *et al*. 2019, Jena *et al*. 2020, Shariati *et al*. 2020, Lyashenko *et al*. 2020).

Shell physical parameters are varied to enhance the strength and stability of a physical system. As dynamical parameters are changed, the shell problem is converted into other one. This amendment leads to explore either a new numerical method or extended to investigate new variations in dynamical characteristics of a shell problem. Analytical characteristics study of shell problems is performed to predict the experimental results. MATLAB codes are used to write programs to observe vibrations of constrained cylindrical shells containing fluid.

2. Theoretical formulation

2.1 Functionally graded materials and volume fraction

Two or more types of materials are used to structure the functionally graded materials (FGMs) by some material allotment law and their physical properties vary from one surface to the other surface. In these surfaces one has highly heat resistance property while other may preserve great dynamical perseverance. So they are materials keeping dually physical appearance. Their material constituent differs in regular comportment from one surface to other surface. Examples of these types of materials are found in nature and contain plants, boons, teeth of our body, coconut shell, bamboos and bio-tissues of animals. All these materials having changeable outer and inner sides and have higher physical properties. These materials are organized by various techniques and their applications are seen in dynamical elements such as plates, beams, shells and more over they are observed space crafts, nuclear reactors and missiles technology etc. Yamanouchi *et al*. (1990) and Koizumi (1993) sheared their ideas to frame these materials. Powder technology is utilized to structure functionally graded materials that can tolerate resistance properties in high temperature.

Various types of volume fraction law is utilized to restrict the material distribution in a functionally graded material. Mathematically, their expressions are written as a polynomial, exponential and trigonometric functions. These functions include the shell thickness variable and some volume exponents that lie between 0 and∞, from these volume fraction laws only exponential volume fraction law is used for the present work.

For a cylindrical shell, the volume fraction of a functionally graded material component depends on thickness variable of the shell and its formula is given as:

$$V_r = \left(\frac{z - R_1}{R_o - R_1}\right)^N \tag{1}$$

where N is the power law exponent and its value lie between zero and infinity. z represent the shell thickness variable quantity and $R_1 \le z \le R_0$ in the radial direction where R_1 and R_0 are the inner and outer radii of the shell. The volume fraction for a functionally graded ingredient material is expressed as:

$$V_r = \left[\frac{2z+h}{2h}\right]^N \tag{2}$$

where *h* stands for the shell uniform thickness.

In practice a cylindrical shell is framed from a FGM which contains of two component materials these are denoted by M_1 and M_2. If E_1 and E_2 as Young's moduli, ν_1 and ν_2 as Poisson's ratios, ρ_1 and ρ_2 mass densities respectively. Then effective material quantities: Young's modulus, E_{FGM}, Poisson's ratio, v_{FGM} and mass density, ρ_{FGM} of the FGM are given as:

$$E_{FGM} = [E_1 - E_2]\left[\frac{2z+h}{2h}\right]^N + E_2 \tag{3}$$

$$v_{FGM} = [v_1 - v_2]\left[\frac{2z+h}{2h}\right]^q + v_2 \tag{4}$$

$$\rho_{FGM} = [\rho_1 - \rho_2]\left[\frac{2z+h}{2h}\right]^q + \rho_2 \tag{5}$$

A material property of a functionally graded material depends on its fabric distribution prearranged by a volume

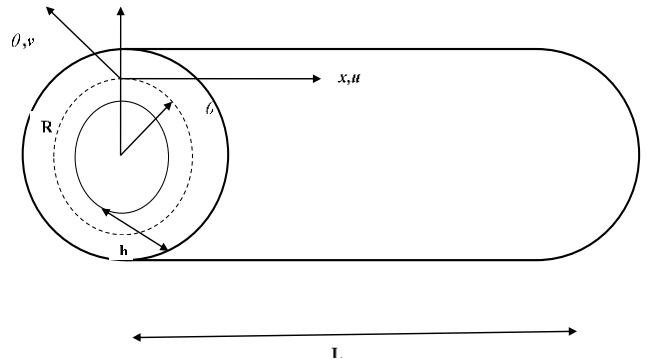

Fig. 1 Geometry of cylindrical shell

fraction law. Arshad *et al*. (2007) devised volume fraction law maintenance the property that the sum of functionally material constituents is unity as:

$$V_r = 1 - e^{-\left(\frac{z}{h}+0.5\right)^N} \tag{6}$$

where e is the paramount irrational number used natural logarithm base and its value is $e = 2.718$.

Therefore, from these expressions, the actual fabric properties: mass density ρ Poisson ratio v, and Young's modulus E, for a functionally graded cylindrical hell are written as:

$$E_{FGM} = (E_1 - E_2)\left(1 - e^{-\left(\frac{z}{h}+0.5\right)^N}\right) + E_2 \tag{7}$$

$$v_{FGM} = (v_1 - v_2)\left(1 - e^{-\left(\frac{z}{h}+0.5\right)^N}\right) + v_2 \tag{8}$$

$$\rho_{FGM} = (\rho_1 - \rho_2)\left(1 - e^{-\left(\frac{z}{h}+0.5\right)^N}\right) + \rho_2 \tag{9}$$

When $z = -\frac{h}{2}$, $E_{FGM} = E_2$, $v_{FGM} = v_2$, and $\rho_{FGM} = \rho_2$, when $z = \frac{h}{2}$, $E_{FGM} = (E_1 - E_2)\left(1 - e^{-1}\right) + E_2$, $v_{FGM} = (v_1 - v_2)(1 - e^{-1}) + v_2$ and $\rho_{FGM} = (\rho_1 - \rho_2)(1 - e^{-1}) + \rho_2$.

These expressions represent that the fabric properties of the constituent material dominate at the shell internal surface while these possessions are the arrangement of the two constituent materials M_1 and M_2 at the shell external surface.

When these expressions are used to evaluate the coupling, membrane, and flexural stiffness, the integrals related to them become burdensome and complex. So, to solve them a numerical integration technique is applied. This technique may take a minute time and effort. To shun this anomalous situation, an approximation regarding the Poisson's ratios for M_1 and M_2 is demoralized. These ratios are taking approximate equal to each other that is,

$$v_1 \simeq v_2 \tag{10}$$

This supposition simplifies the procedure of evaluation of integrals denoting material stiffness moduli. A functionally graded cylindrical shell consisting of two ingredient materials can be divided into two types. In these categories nickel and stainless steel are used as the interior surfaces and the exterior surface but their arrangement has paramount influence on the formation of cylindrical shell in the presence of functionally graded materials. The order of the functionally graded constituent materials is reversed with regard to category I and category II. This categorization is given below and material characteristics of functionally graded materials: nickel and stainless steel are expressed in Table 1.

The x, θ co-ordinate are assumed to be along longitudinal and circumferential direction, respectively and z - co-ordinates are taken in its radial directions. The reference surface is setup as an orthogonal system (x, θ, t) as shown in Fig. 1.

According to Love shell theory, the governing equations of cylindrical shell are

$$\varsigma_{11}u + \varsigma_{12}v + \varsigma_{13}w = \rho h\frac{\partial^2 u}{\partial t^2} \tag{11}$$

$$\varsigma_{21}u + \varsigma_{22}v + \varsigma_{23}w = \rho h\frac{\partial^2 v}{\partial t^2} \tag{12}$$

$$\varsigma_{31}u + \varsigma_{32}v + \varsigma_{33}w = \rho h\frac{\partial^2 w}{\partial t^2} \tag{13}$$

where the operators $\varsigma_{i_j}'s(i,j = 1,2,3)$ are the differential operators involving the variable x and θ. Furthermore, full form of these equations are

$$A_{11}\frac{\partial^2 u}{\partial x^2} + \frac{A_{66}}{R^2}\frac{\partial^2 u}{\partial \theta^2} + \left(\frac{A_{12}+A_{66}}{R} + \frac{B_{12}+2B_{66}}{R^2}\right)\frac{\partial^2 v}{\partial x \partial \theta} + \frac{A_{12}}{R}\frac{\partial w}{\partial x} - B_{11}\frac{\partial^3 w}{\partial x^3} - \frac{B_{12}+2B_{66}}{R^2}\frac{\partial^3 w}{\partial x \partial \theta^2} = \rho h\frac{\partial^2 u}{\partial t^2} \tag{14}$$

$$\left(\frac{A_{12}+A_{66}}{R} + \frac{B_{12}+B_{66}}{R^2}\right)\frac{\partial^2 u}{\partial x \partial \theta} + \left(A_{66} + \frac{3B_{66}}{R} + \frac{3D_{66}}{R^2}\right)\frac{\partial^2 v}{\partial x^2} + \left(\frac{A_{22}}{R^2} + \frac{2B_{22}}{R^3} + \frac{D_{22}}{R^4}\right)\frac{\partial^2 v}{\partial \theta^2} - \left(\frac{B_{12}+2B_{66}}{R} + \frac{D_{12}+2D_{66}}{R^2}\right)\frac{\partial^3 w}{\partial x^2 \partial \theta} + \left(\frac{A_{22}}{R^2} + \frac{B_{22}}{R^3}\right)\frac{\partial w}{\partial \theta} - \left(\frac{B_{22}}{R^3} + \frac{D_{22}}{R^4}\right)\frac{\partial^3 w}{\partial \theta^3} = \rho h\frac{\partial^2 v}{\partial t^2} \tag{15}$$

$$B_{11}\frac{\partial^3 u}{\partial x^3} - \frac{A_{12}}{R}\frac{\partial u}{\partial x} + \frac{B_{12}+2B_{66}}{R^2}\frac{\partial^3 u}{\partial x \partial \theta^2} + \left(\frac{B_{12}+2B_{66}}{R} + \frac{D_{12}+4D_{66}}{R^2}\right)\frac{\partial^3 v}{\partial x^2 \partial \theta} + \left(\frac{B_{22}}{R^3} + \frac{D_{22}}{R^4}\right)\frac{\partial^3 v}{\partial \theta^3} - \left(\frac{A_{22}}{R^2} + \frac{B_{22}}{R^3}\right)\frac{\partial v}{\partial \theta} - D_{11}\frac{\partial^4 w}{\partial x^4} - \frac{2(D_{12}+2D_{66})}{R^2}\frac{\partial^4 w}{\partial x^2 \partial \theta^2} - \frac{D_{22}}{R^4}\frac{\partial^4 w}{\partial \theta^4} + \frac{2B_{12}}{R}\frac{\partial^2 w}{\partial x^2} + \frac{2B_{22}}{R^3}\frac{\partial^2 w}{\partial \theta^2} - \frac{A_{22}}{R^2}w = \rho h\frac{\partial^2 w}{\partial t^2} \tag{16}$$

Here, ρ denotes density and expressed as where A_{ij}, B_{ij} and $D_{ij}(i,j = 1,2,6)$ denote the extensional, coupling and bending stiffness respectively and are defined as:

$$A_{ij} = \int_{\frac{-h}{2}}^{\frac{h}{2}} Q_{ij}\, dz \tag{17}$$

$$B_{ij} = \int_{\frac{-h}{2}}^{\frac{h}{2}} Q_{ij} z d\, z \tag{18}$$

$$D_{ij} = \int_{\frac{-h}{2}}^{\frac{h}{2}} Q_{ij}\, z^2 dz \tag{19}$$

and the membrane (A_{ij}), coupling (B_{ij}) and flexural (D_{ij}) respectively for exponential volume fraction law are expressed as:

$$\begin{Bmatrix} A_{11} = \frac{1}{1-{v_1}^2}\int_{-\frac{h}{2}}^{\frac{h}{2}}\left[(E_1-E_2)\left(1-e^{-(\frac{z}{h}+0.5)^q}\right)+E_2\right]dz, \\ A_{12} = \frac{v_1}{1-{v_1}^2}\int_{-\frac{h}{2}}^{\frac{h}{2}}\left[(E_1-E_2)\left(1-e^{-(\frac{z}{h}+0.5)^q}\right)+E_2\right]dz \\ A_{11} = A_{22}, \\ A_{66} = \frac{0.5}{1+v_1}\int_{-\frac{h}{2}}^{\frac{h}{2}}\left[(E_1-E_2)\left(1-e^{-(\frac{z}{h}+0.5)^q}\right)+E_2\right]dz \end{Bmatrix} \tag{20}$$

$$\begin{Bmatrix} B_{11} = \frac{1}{1-{v_1}^2}\int_{-\frac{h}{2}}^{\frac{h}{2}}\left[(E_1-E_2)\left(1-e^{-(\frac{z}{h}+0.5)^q}\right)+E_2\right]zdz, \\ B_{12} = \frac{v_1}{1-{v_1}^2}\int_{-\frac{h}{2}}^{\frac{h}{2}}\left[(E_1-E_2)\left(1-e^{-(\frac{z}{h}+0.5)^q}\right)+E_2\right]zdz \\ B_{11} = B_{22}, \\ B_{66} = \frac{0.5}{1+v_1}\int_{-\frac{h}{2}}^{\frac{h}{2}}\left[(E_1-E_2)\left(1-e^{-(\frac{z}{h}+0.5)^q}\right)+E_2\right]zdz \end{Bmatrix} \tag{21}$$

$$\begin{Bmatrix} D_{11} = \frac{1}{1-{v_1}^2}\int_{-\frac{h}{2}}^{\frac{h}{2}}\left[(E_1-E_2)\left(1-e^{-(\frac{z}{h}+0.5)^q}\right)+E_2\right]z^2dz, \\ D_{12} = \frac{v_1}{1-{v_1}^2}\int_{-\frac{h}{2}}^{\frac{h}{2}}\left[(E_1-E_2)\left(1-e^{-(\frac{z}{h}+0.5)^q}\right)+E_2\right]z^2dz \\ D_{11} = D_{22}, \\ D_{66} = \frac{0.5}{1+v_1}\int_{-\frac{h}{2}}^{\frac{h}{2}}\left[(E_1-E_2)\left(1-e^{-(\frac{z}{h}+0.5)^q}\right)+E_2\right]z^2dz \end{Bmatrix} \tag{22}$$

Space variables x, θ and time variable *t*, are separated from the equations of displacements deformation functions that are also used in kinetic and strain energy relations. In shell equations these functions are substituted and then by applying Galerkin approach a system of differential equations is obtained that contain three unknown dependent variables. These equations are expressed as:

$$u(x,\theta,t) = A\frac{d\varphi}{dx} sin\, n\,\theta\, sin\,\omega\, t \tag{23}$$

$$v(x,\theta,t) = B\varphi(x)\, cos\, n\,\theta\, sin\,\omega\, t \tag{24}$$

$$w(x,\theta,t) = C\varphi\sum_{i=1}^{k}(x-a_i)^k\, sin\, n\,\theta\, sin\,\omega\, t \tag{25}$$

A, B and C are the constants that represents the amplitudes of vibrations and n is the circumferential wave number, and m is the axial wave number and natural circular frequency for a cylindrical shell is denoted by $\omega(rad^{-1})$. Axial modal deformation functions $U(x)$, $V(x)$ and $W(x)$ are defined in the longitudinal, tangential and transverse directions and they also meet boundary conditions. The Galerkin technique is used to solve the shell governing equations. For this purpose, the modal displacement forms for *u*, *v* and *w* given in the relation Eqs. (23)-(25) in the Eqs. (14)-(16) respectively and their corresponding partial derivatives are substituted into the equations (4.8a) – (4.8c) and the outcomes of equations are multiplied by $U(x)$, $V(x)$ and $W(x)$ respectively. The resulting equations are integrated with respect to *x* from 0 to *L*, the following equations are obtained.

The arranged term to form the homogeneous algebraic linear equations in *A*, *B* and *C* as

$$\begin{aligned} \boldsymbol{\varsigma_{11}A + \varsigma_{12}B + \varsigma_{13}C} &= \boldsymbol{-\omega^2\rho hAI_2} \\ \boldsymbol{\varsigma_{21}A + \varsigma_{22}B + \varsigma_{23}C} &= \boldsymbol{-\omega^2\rho hBI_2} \\ \boldsymbol{\varsigma_{31}A + \varsigma_{32}B + \varsigma_{33}C} &= \boldsymbol{-\omega^2\rho hCI_2} \end{aligned} \tag{26}$$

where $\varsigma_{ij}(i,j = 1,2,3)$ are the quantities implicating the shell parameters. This is an eigen-value problem involving the shell frequency. There are various computer software to solve such problems. The software MATLAB is preferred to others because of convenient computing coding. Evaluation of physical problems in engineering and science is widely done by MATLAB. Just single command 'eig' furnishes shell frequencies and mode shapes by calculating eigenvalues and eigenvectors respectively.

3. Equilibrium equations for Nanobeams

A few comparisons of analytical frequencies for isotropic cylindrical shells are exhibited to validate the present Galerkin procedure. Table 1 shows dimensionless frequency parameters $\Omega = \omega R\sqrt{(1-\nu^2)\rho/E}$ for a simply supported cylindrical shell. They are varied with circumferential wave mode, n for the axial wave number, *m* = 1. They are compared with those ones by Loy *et al.* (1997). Loy *et al.* (1997) used the generalized differential quadrature method to find the frequency parameters. A good agreement is seen between two sets of the frequency parameters. Table 2 displays a comparison of dimensionless frequency parameters for a simply supported cylindrical shell on both ends. They are compared with ones found by Naeem and Sharma (2000). The half-longitudinal wave mode, *m* is equal to unity. Here the trigonometric functions are used for the axial deformation functions and the Galerkin procedure is applied to derive shell frequency while Naeem and Sharma (2000) employed the Rayleigh-Ritz formulation with the Ritz polynomial function for the axial modal displacements. There has been found a good agreement between two sets of frequencies. In Table 3 comparison of variations of natural frequencies (Hz) for cylindrical shells is presented with the circumferential wave mode (*n*). An observation is made that the frequencies related to a cylindrical shell are highly lessened when they are compared with those determined for an empty cylindrical shell with same shell quantities. The lowest frequency corresponds to *n* = 3. In Table 4 natural

Table 1 Comparison of frequency parameter $\Omega = \omega R\sqrt{(1-\nu^2)\rho/E}$ for a simply supported cylindrical shell ($m = 1,\ L/R = 20,\ h/R = 0.01,\ \nu = 0.3$)

n	Loy *et al*.(1997)	Present
1	0.016101	0.016102
2	0.009382	0.009383
3	0.022105	0.022106
4	0.042095	0.042097
5	0.068008	0.068009

Table 2 Comparison of dimensionless frequency parameter Ω for a simply supported cylindrical shell ($m = 1, L/R = 6, h/R = 0.002, R = 1, \nu = 0.3$)

n	Naeem and Sharma (2000)	Present
6	0.021303	0.021304
7	0.028089	0.028087
8	0.036469	0.036467
9	0.046174	0.046170
10	0.057088	0.057087

Table 3 Comparison of frequencies (Hz) for simply supported cylindrical shell($m = 1,\ L/R = 20,\ \frac{h}{R} = 0.002$)

Frequencies (HZ)	N	Method	n				
			1	2	3	4	5
	0.3	Iqbal *et al*. (2009)	13.038	4.4159	4.094	6.939	11.0868
		Present	13.038	4.4174	4.0942	6.9358	11.0798

Table 4 Variations of natural frequencies (Hz) against circumferential wave number n for FGM cylindrical shells with ring support. Category-II (m = 1, L = 8m, h = 0.004m, R = 1m, N = 0.5)

n	a = 0.1L	
	Frequency without ring support	Frequency with ring support
1	243.246	161.09
2	305.194	198.733
3	322.211	210.06
4	328.6	214.393
5	331.619	216.462
6	333.261	217.647
7	334.241	218.301
8	334.861	218.749
9	335.269	219.001
10	335.543	219.209

frequencies (Hz) for FGM cylindrical shells: Type-II without and with ring supports are listed with the circumferential wave number, n. The ring supports are maintained at the location a = 0.1L, 0.5L, L. Like Type-I cylindrical shells, frequencies increase indefinitely with n

Table 5 Variation of natural frequencies (Hz) versus the position of ring supports for FGM cylindrical shell with ring supports. (n = 1, m = 1, L = 8m, h = 0.004m, R = 1m)

a	Frequency (Hz)
0	204.048
0.1L	243.246
0.2L	301.997
0.3L	390.677
0.4L	487.212
0.5L	513.823
0.6L	487.212
0.7L	390.677
0.8L	301.997
0.9L	243.246
L	204.048

for every location of the ring support. Minimum frequency is found to be related with n = 1 the cylindrical shells with and without rings. Again there are substantial decrements in the shell frequencies due to inclusion of fluid loaded terms. Table 5 display the variations of natural frequencies (Hz) for FGM cylindrical shells. They are varied against the locations of the ring supports. The frequencies first rise, attain their maximum at the mid position and then fall down to original values at the other shell end. Fig. 2 show the frequency variations of Type-I clamped simply supported FG cylindrical shell with different positions of ring supports a = 0.0, 0.2, 0.4 against the circumferential wave number, n = 1 ~ 10. The value of exponent of exponential law N is fixed to 0.5. The frequencies for ring supports a = 0.1, 0.2, 0.4 at n = 1 having minute difference and the gap between the frequency curves is small. As progressing the circumferential wave number, the frequencies increases and gap between the frequency curves is also in increasing mode. The ring supports a = 0.0 having low frequencies then other ring supports a = 0.2, 0.4. The behavior of gap between curves increases suddenly after circumferential wave number.

The values of frequencies of ring support a = 0.2 is sandwiched between two remaining ring supports. Figs 3 depict the natural frequencies of Type-II cylindrical shells versus circumferential wave mode, n for the half - axial wave mode, m = 1 and exponent of exponential law N is fixed to 0.5. The shells are supported by the ring supports at various positions. Distribution of the functionally graded material in the transverse direction is managed by the exponential fraction law. It is witnessed that the effects of the ring supports on the shell vibration frequency is very pronounced again the circumferential wave numbers n. As n is enhanced, the frequency increases with n. The frequencies of ring support a = 0.4 is higher than that of a = 0.0, 0.2. It can be seen that the frequencies of Type-II is less than that of Type-I. The distribution of the material can be seen in the Table 1. In Figs. 4 and 5, variations of natural frequencies (Hz) for Type-I and Type-II functionally graded cylindrical shells are plotted for exponential volume fraction law. The

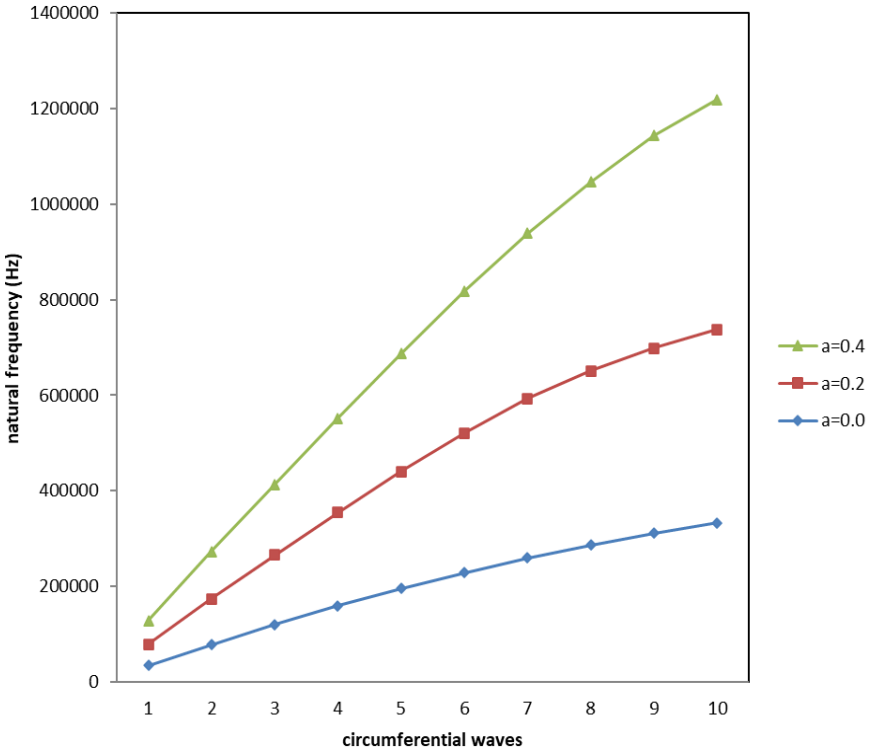

Fig. 2 Variations of frequencies of Type-I clamped simply supported cylindrical shell against $n(m = 1, L = 20, R = 1, h = 0.002)$

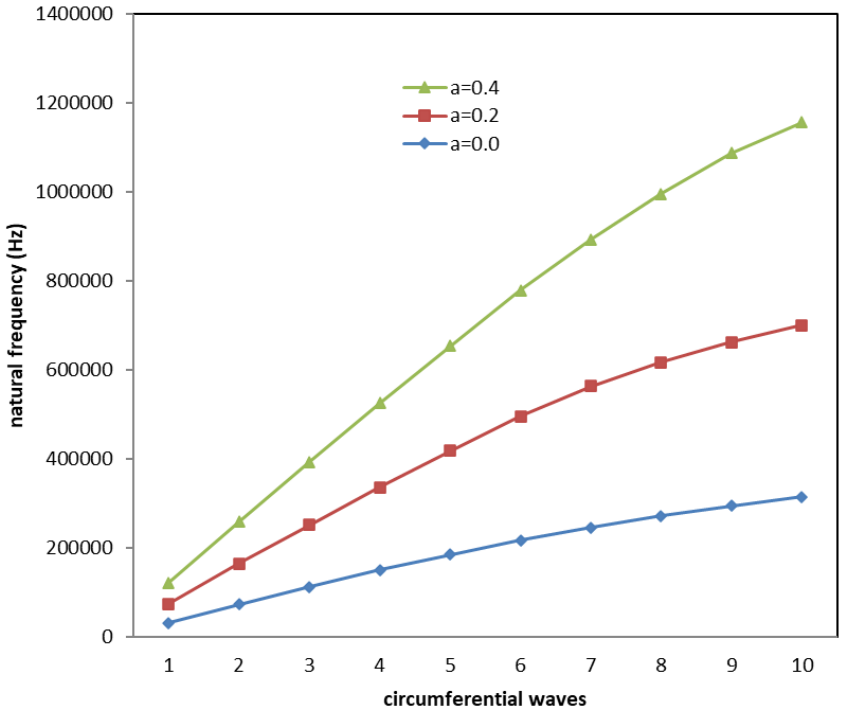

Fig. 3 Variations of frequencies of Type-II clamped simply supported cylindrical shell against $n(m = 1, L = 20, R = 1, h = 0.002)$

behavior of exponent of volume fraction law N is seen for three different values as 0.5, 1, 2. In these figures, frequencies (Hz) of Type-I and II clamped simply supported cylindrical shells are given against, n for the axial wave number, m = 1 with ring support respectively. The ring support is attached at a = 0.5. The results are evaluated by applying the polynomial volume fraction law. It is noticed that as n is increased, the frequency increases and the minimum frequency is associated with the circumferential wave number, n = 1. But the frequency variations with volume fraction exponents N have similar behavior as with the circumferential wave number frequency increases as N

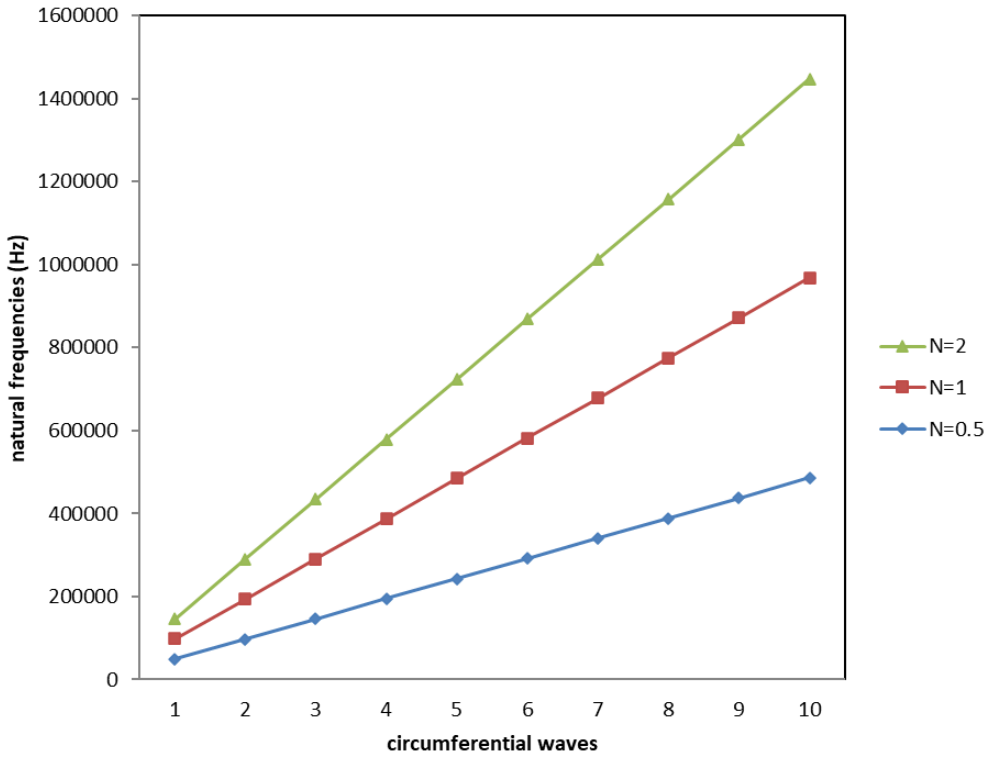

Fig. 4 Variations of frequencies of Type-I clamped simply supported cylindrical shell with ring support, against n. $(m = 1, L = 20, R = 1, a = 0.5, h = 0.002)$

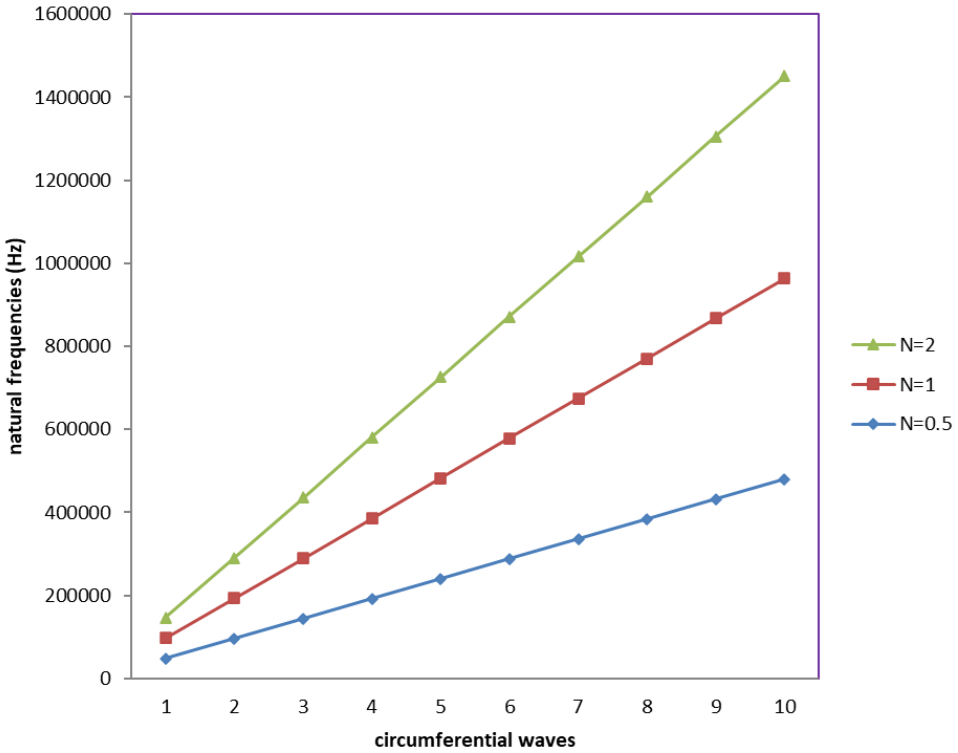

Fig. 5 Variations of frequencies of Type-II clamped simply supported cylindrical shell with ring support, against n.$(m = 1, L = 20, R = 1, a = 0.5, h = 0.002)$

is increased. But in the two cases, the frequency values lie between those values of the cylindrical shells consisting of only nickel or stainless steel materials. Similarly the frequencies are determined. Type 1 cylindrical shells, frequency values are the highest exponent of volume fraction law N. In case of Type-I cylindrical shells, natural frequencies for the exponent of volume fraction law N are the lowest.

4. Conclusions

In this study, frequency analysis for functionally graded cylindrical is performed by attaching some ring supports. These rings are located at some distance from one end of a cylindrical shell. Before applying this technique, the classical method of separation of variables for PDEs is engaged to split spacial and temporal variables is applied. This process gives birth a set of three ODEs. The functions of space variable and their ordinary derivatives are involved with shell physical quantities. These functions depend on the axial variable and are assumed by some appropriate mathematical ones which ensure to meet the edge conditions. These functions may the characteristic beam functions or polynomials or circular functions or exponential functions. This assumption is called the axial modal dependence. The characteristic beam functions are the eigen – functions evaluated from solutions of the differential equation representing vibration of a beam. The ring support is attached at $a = 0.5$. The results are evaluated by applying the polynomial volume fraction law. Type 1 cylindrical shells, frequency values are the highest exponent of volume fraction law *N*. In case of Type-II cylindrical shells, natural frequencies for the exponent of volume fraction law *N* are the lowest. This model can be extended for the vibration of nano-shells

Acknowledgments

This research work was funded by Institutional Fund Projects under grant no. (IFPIP-238-980-1443). Therefore, authors gratefully acknowledge the technical and financial support from the Ministry of Education and King Abdulaziz University, DSR, Jeddah, Saudi Arabia.

References

Abouelregal, A.E., Mohammed, W.W. and Mohammad-Sedighi, H. (2021), "Vibration analysis of functionally graded micro-beam under initial stress via a generalized thermoelastic model with dual-phase lags", *Arch. Appl. Mech.*, **91**(5), 2127-2142. https://doi.org/10.1007/s00419-020-01873-2.

Abouelregal, A.E. and Sedighi, H.M. (2021), "The effect of variable properties and rotation in a visco-thermoelastic orthotropic annular cylinder under the Moore–Gibson–Thompson heat conduction model", *Proceedings of the Institution of Mechanical Engineers, Part L: Journal of Materials: Design and Applications*, **235**(5), 1004-1020.

Akbaş, Ş.D. (2016a), "Forced vibration analysis of viscoelastic nanobeams embedded in an elastic medium", *Smart Struct. Syst.*, **18**(6), 1125-1143. https://doi.org/10.12989/sss.2016.18.6.1125.

Akbaş, Ş.D. (2016b), "Analytical solutions for static bending of edge cracked micro beams", *Struct. Eng. Mech.*, **59**(3), 579-599. https://doi.org/10.12989/sem.2016.59.3.579.

Akbaş Ş.D. (2017a), "Free vibration of edge cracked functionally graded microscale beams based on the modified couple stress theory", *Int. J. Struct. Stabil. Dyn.*, **17**(3), 1750033. https://doi.org/10.1142/S021945541750033X.

Akbaş, Ş.D. (2017b), "Forced vibration analysis of functionally graded nanobeams", *Int. J. Appl. Mech.*, **9**(7), 1750100. https://doi.org/10.1142/S1758825117501009.

Akbas, S.D. (2018a), "Forced vibration analysis of cracked functionally graded microbeams", *Adv. Nano Res.*, **6**(1), 39-55. https://doi.org/10.12989/anr.2018.6.1.039.

Akbaş, Ş.D. (2018b), "Bending of a cracked functionally graded nanobeam", *Adv. Nano Res.*, **6**(3), 219-243. https://doi.org/10.12989/anr.2018.6.3.219.

Akbaş, Ş.D. (2018c), "Forced vibration analysis of cracked nanobeams", *J. Brazil. Soc. Mech. Sci. Eng.*, **40**(8), 1-11. https://doi.org/10.1007/s40430-018-1315-1.

Akbaş, Ş.D. (2019), "Axially forced vibration analysis of cracked a nanorod", *J. Comput. Appl. Mech.*, **50**(1), 63-68. https://doi.org/10.22059/JCAMECH.2019.281285.392.

Akbaş, Ş.D. (2020), "Modal analysis of viscoelastic nanorods under an axially harmonic load", *Adv. Nano Res.*, **8**(4), 277-282. https://doi.org/10.12989/anr.2020.8.4.277.

Benmansour, D.L., Kaci, A., Bousahla, A.A., Heireche, H., Tounsi, A., Alwabli, A.S., ... and Mahmoud, S.R. (2019), "The nano scale bending and dynamic properties of isolated protein microtubules based on modified strain gradient theory", *Adv. Nano Res.*, **7**(6), 443-457. https://doi.org/10.12989/anr.2019.7.6.443.

Civalek, Ö. (2020), "Vibration of functionally graded carbon nanotube reinforced quadrilateral plates using geometric transformation discrete singular convolution method", *Int. J. Numer. Meth. Eng.*, **121**(5), 990-1019. https://doi.org/10.1002/nme.625.

Civalek, O. and Jalaei, M.H. (2020). "Buckling of carbon nanotube (CNT)-reinforced composite skew plates by the discrete singular convolution method", *Acta Mechanica*, **231**(6), 2565-2587. https://doi.org/10.1002/nme.6254.

Ebrahimi, F., Dabbagh, A., Rabczuk, T. and Tornabene, F. (2019), "Analysis of propagation characteristics of elastic waves in heterogeneous nanobeams employing a new two-step porosity-dependent homogenization scheme", *Adv. Nano Res.*, **7**(2), 135-143. https://doi.org/10.12989/anr.2019.7.2.135.

Eltaher, M.A., Almalki, T.A., Ahmed, K.I. and Almitani, K.H. (2019), "Characterization and behaviors of single walled carbon nanotube by equivalent-continuum mechanics approach", *Adv. Nano Res.*, **7**(1), 39. https://doi.org/10.12989/anr.2019.7.1.039.

Ergin, A. and Temarel, P. (2002), "Free vibration of a partially liquid-filled and submerged, horizontal cylindrical shell", *J. Sound Vib.*, **254**(5), 951-965. https://doi.org/10.1006/jsvi.2001.4139.

Greif, R and Chung, H. (1975), "Vibration of constrained cylindrical shells", *Am. Inst. Aeronaut. J.*, **13**, 1190-1198. https://doi.org/10.2514/3.6970.

Iqbal, Z., Naeem, M.N., Sultana, N., Arshad, S.H. and Shah, A.G. (2009), "Vibration characteristics of FGM circular cylindrical shells filled with fluid using wave propagation approach", *Appl. Math. Mech.*, **30**, 1393-1404. https://doi.org/10.1007/s10483-009-1105-x.

Jena, S.K., Chakraverty, S., Malikan, M. and Sedighi, H. (2020), "Implementation of Hermite–Ritz method and Navier's technique for vibration of functionally graded porous nanobeam embedded in Winkler–Pasternak elastic foundation using bi-Helmholtz nonlocal elasticity", *J. Mech. Mater. Struct.*, **15**(3), 405-434. https://doi.org/10.2140/jomms.2020.15.405.

Koochi, A. and Goharimanesh, M. (2021), "Nonlinear oscillations of CNT nano-resonator based on nonlocal elasticity: The energy balance method", *Reports Mech. Eng.*, **2**(1), 41-50. https://doi.org/10.31181/rme200102041g.

Loy, C.T. and Lam, K.Y. (1997), "Vibration of cylindrical shells with ring supports", *J. Mech. Eng.*, **39**, 455-471. https://doi.org/10.1016/S0020-7403(96)00035-5.

Loy, C.T. Lam, K.Y. and Reddy, J.N. (1999), "Vibration of functionally graded cylindrical shells", *Int. J. Mech. Sci.*, **41**,

309-324. https://doi.org/10.1016/S0020-7403(98)00054-X
Ludwig, A. and R. Krieg (1981), "An analytical Quasi-exact method for calculating eigen vibrations of thin circular cylindrical shells", *J. Sound Vib*., **74**, 155-174. https://doi.org/10.1016/0022-460X(81)90501-0.
Lyashenko, I.A., Borysiuk, V.N. and Popov, V.L. (2020), "Dynamical model of the asymmetric actuator of directional motion based on power-law graded materials", **18**(2), 245-254. https://doi.org/10.22190/FUME200129020L.
Naeem, M.N. and Sharma, C.B. (2000), "Prediction of natural-frequencies for thin circular cylindrical shells", *Proc. Inst. Mech*., **214**(10), 1313-1328. https://doi.org/10.1243/0954406001523290.
Safaei, B., Khoda, F.H. and Fattahi, A.M. (2019), "Non-classical plate model for single-layered graphene sheet for axial buckling", *Adv. Nano Res*., **7**(4), 265-275. https://doi.org/10.12989/anr.2019.7.4.265.
Sarkheil, S., Foumani, M.S. and Navazi. H.M (2016), "Free vibration of bi-material cylindrical shells", *Proceedings of the Institution of Mechanical Engineers, Part C: Journal of Mechanical Engineering Science*, **230**, 2637-2649. https://doi.org/10.1177/0954406215602037
Shahsavari, D., Karami, B. and Janghorban, M. (2019), "Size-dependent vibration analysis of laminated composite plates", *Adv. Nano Res*., **7**(5), 337-349. https://doi.org/10.12989/anr.2019.7.5.337.
Shariati, A., Jung, D.W., Mohammad-Sedighi, H., Żur, K.K., Habibi, M. and Safa, M. (2020), "On the vibrations and stability of moving viscoelastic axially functionally graded nanobeams", *Materials*, **13**(7), 1707. https://doi.org/10.3390/ma13071707.
Swaddiwudhipong, S., Tian, J. and Wang, C.M. (1995), "Vibrations of cylindrical shells with intermediate supports", *J. Sound Vib*., **187**(1), 69-93. https://doi.org/10.1006/jsvi.1995.0503.
Wang, C., and Lai, J.C.S. (2000), "Prediction of natural frequencies of finite length circular cylindrical shells", *Appl. Acoust*., **59**(4), 385-400. https://doi.org/10.1016/S0003-682X(99)00039-0.
Zhang, L., Xiang, Y. and Wei, G.W. (2006), "Local adaptive differential quadrature for free vibration analysis of cylindrical shells with various boundary conditions", *Int. J. Mech. Sci*., **48**, 1126-1138. https://doi.org/10.1016/j.ijmecsci.2006.05.005.

CC

Appendix I

$$\varsigma_{11} = A_{11}I_1 - n^2\frac{A_{66}}{R^2}I_2$$
$$\varsigma_{12} = -\left(\frac{A_{12}+A_{66}}{R} + \frac{B_{12}+2B_{66}}{R^2}\right)I_3$$
$$\varsigma_{13} = \left(\frac{A_{12}}{R} + n^2\frac{B_{12}+2B_{66}}{R^2}\right)I_3 - B_{11}I_4$$
$$\varsigma_{21} = n\left(\frac{A_{12}+A_{66}}{R} + \frac{B_{12}+B_{66}}{R^2}\right)I_5$$
$$\varsigma_{22} = \left(A_{66} + \frac{3B_{66}}{R} + \frac{3D_{66}}{R^2}\right)I_1 - n^2\left(\frac{A_{66}}{R^2} + \frac{2B_{22}}{R^3} + \frac{D_{22}}{R^4}\right)I_2$$
$$\varsigma_{23} = -\left(\frac{B_{12}+2B_{66}}{R} + \frac{D_{12}+2D_{66}}{R^2}\right)nI_1$$
$$+I_2\left\{\left(\frac{A_{22}}{R^2} - \frac{B_{22}}{R^3}\right)n + \left(\frac{B_{22}}{R^3} + \frac{D_{22}}{R^4}\right)n^3\right\}$$
$$\varsigma_{31} = -\frac{A_{12}}{R}I_5 + B_{11}I_6 - n^2\frac{B_{12}+2B_{66}}{R^2}I_5$$
$$\varsigma_{32} = n\left(\frac{A_{22}}{R^2} + \frac{B_{22}}{R^3}\right)I_2 + n^3\left(\frac{B_{22}}{R^3} + \frac{D_{22}}{R^4}\right)I_2$$
$$-n\left(\frac{B_{12}+2B_{66}}{R} + \frac{D_{12}+4D_{66}}{R^2}\right)I_1$$
$$\varsigma_{33} = I_1\left\{\frac{2(D_{12}+2D_{66})}{R^2}n^2 + \frac{B_{12}}{R}\right\}$$
$$-\left(\frac{D_{22}n^4}{R^4} + \frac{2B_{22}n^2}{R^3} + \frac{A_{22}}{R}\right)I_2 - D_{11}I_7$$

Appendix II

$$I_1 = -m^2\pi^2/2L$$
$$I_2 = L/2$$
$$I_3 = m\pi/2$$
$$I_4 = -m^3\pi^3/2L^2$$
$$I_5 = -m\pi/2$$
$$I_6 = m^3\pi^3/2L^2$$
$$I_7 = m^4\pi^4/2L^3$$